On the performance of molecular polarization methods. II. Water and carbon tetrachloride close to a cation

Marco Masia[a)]
Departament de Física i Enginyeria Nuclear, Universitat Politècnica de Catalunya, Campus Nord B4-B5, Barcelona 08034, Spain

Michael Probst[b)]
Institute of Ion Physics, Universität Innsbruck, Technikerstrasse 25, Innsbruck A-6020, Austria

Rossend Rey[c)]
Departament de Física i Enginyeria Nuclear, Universitat Politècnica de Catalunya, Campus Nord B4-B5, Barcelona 08034, Spain

(Received 30 June 2005; accepted 24 August 2005; published online 25 October 2005)

Our initial study on the performance of molecular polarization methods close to a positive point charge [M. Masia, M. Probst, and R. Rey, J. Chem. Phys. **121**, 7362 (2004)] is extended to the case in which a molecule interacts with a real cation. Two different methods (point dipoles and shell model) are applied to both the ion and the molecule. The results are tested against high-level *ab initio* calculations for a molecule (water or carbon tetrachloride) close to Li^+, Na^+, Mg^{2+}, and Ca^{2+}. The monitored observable is in all cases the dimer electric dipole as a function of the ion-molecule distance for selected molecular orientations. The moderate disagreement previously obtained for point charges at intermediate distances, and attributed to the linearity of current polarization methods (as opposed to the nonlinear effects evident in *ab initio* calculations), is confirmed for real cations as well. More importantly, it is found that at short separations the phenomenological polarization methods studied here substantially overestimate the dipole moment induced if the ion is described quantum chemically as well, in contrast to the dipole moment induced by a point-charge ion, for which they show a better degree of accord with *ab initio* results. Such behavior can be understood in terms of a decrease of atomic polarizabilities due to the repulsion between electronic charge distributions at contact separations. It is shown that a reparametrization of the Thole method for damping of the electric field, used in conjunction with any polarization scheme, allows to satisfactorily reproduce the dimer dipole at short distances. In contrast with the original approach (developed for intramolecular interactions), the present reparametrization is ion and method dependent, and corresponding parameters are given for each case. © *2005 American Institute of Physics*. [DOI: 10.1063/1.2075107]

I. INTRODUCTION

Molecular polarization methods play a central role in the next generation of force fields for molecular simulations[1–5] and much effort is being devoted to the development of methods and parameters.[6–53] This is mainly due to the fact that it is increasingly important to simulate heterogeneous environments, which requires that a given molecular model is able to provide an environment-dependent response. For example, it seems clear that modeling a water molecule with fixed point charges is not adequate to simultaneously describe bulk water molecules and those close to hydrophilic or hydrophobic sites. This is more critical if it is considered that a given molecule may visit these environments within the course of the simulation. Therefore, the inclusion of molecular polarizability seems a basic requirement in order to develop transferable force fields.

Several, rather different, computational approaches have been devised to take into account molecular (and atomic) polarizability. In all cases they are constructed to reproduce the molecular response under homogeneous fields, and are therefore indistinguishable at long intermolecular distances. However, at the short separations typical of a liquid state simulation it is not clear whether they are still interchangeable, as they can have different responses to nonhomogeneous fields. While computational convenience has been a major factor to decide which method to use, it is important to investigate if performance at short distances could be a relevant factor. More important might be the fact that all these methods share a common characteristic: they basically are linear methods and as such they can be expected to fail as nonlinear effects become important. In the simple case study of a point-charge-molecule interaction this was demonstrated to occur at intermediate distances: as the molecule approaches the increasing electric field of the charge[47,53] polarization methods consistently underestimate the induced dipole. It will be shown in this paper that as the distance is further reduced (to values typical of first solvation shell molecules) different nonlinear effects set in due to electronic

[a)]Electronic mail: marco.masia@upc.edu
[b)]Electronic mail: michael.probst@uibk.ac.at
[c)]Electronic mail: rosendo.rey@upc.edu

TABLE I. Water molecule parameters for the methods studied. The polarizability tensor components of model PD2-H_2O are equal to the experimental ones. For the meaning of geometrical parameters we refer to Fig. 2.

	Point dipoles			Shell model	
	PDM	PD1-H_2O	PD2-H_2O		SH-H_2O
d_{OH} (Å)	0.9572	0.9572	0.9572	d_{OH} (Å)	0.9572
d_{OM} (Å)	0.215	0.22	0.0606	d_{OM} (Å)	0.215
θ (degrees)	104.52	104.52	104.52	θ (degrees)	104.52
α_M (Å^3)	1.444	1.420 48	1.4099	k_M (kJ mol^{-1} Å^2)	62 597.64
α_H (Å^3)	0.0	0.001 92	0.0038	k_H (kJ mol^{-1} Å^2)	29 096.44
$\bar{\alpha}$ (Å^3)	1.44	1.47	1.47	$q_{DM}(e)$	8.0
α_{xx} (Å^3)	1.44	1.428	1.415	$q_{DM}(e)$	0.2
α_{yy} (Å^3)	1.44	1.532	1.528		
α_{zz} (Å^3)	1.44	1.451	1.468		

cloud overlapping. This aspect, which obviously could not be addressed for point-charge models, will be central to the present work. The problem here is just the opposite; polarization methods overestimate the induced dipole as they tend to diverge for decreasing ion-molecule separation, while in the real system there is a decrease of induced dipoles.

In our previous studies[47,53] we investigated how the most popular polarization methods perform for water or carbon tetrachloride near a mono- or bivalent positive point charge. These two molecules were chosen for their almost complementary electrostatic properties. Water is a polar molecule with a moderate anisotropic polarizability [$\bar{\alpha}$=1.47 Å^3], while CCl_4 is an apolar molecule with a high isotropic polarizability [α=10.5 Å^3]. For these two molecules, we found that simple point dipoles (PD) and shell (SH) models available in the literature are the best approaches to reproduce the induced dipole moments (although in some cases they required parameter refitting). Fluctuating charge (FQ) models with charges (only) on each atomic site showed a poorer performance. In Tables I and II we give a brief description of the best models for both molecules and methods. It is interesting to note that for water a description with a single point dipole [a model termed point-dipole model (PDM), see Ref. 27], although characterized by an isotropic polarizability, is the one that works best in the case of point charges. In general terms, the main conclusion was that for the important case of singly charged ions in water the phenomenological models produced acceptable results for all distances. This satisfactory behavior is progressively lost as the ion charge and/or molecular polarizability are/is increased.

With this contribution, we look into the limits of molecular polarization models when the molecule interacts with a polarizable cation instead of a point charge. Since the ions also polarize, the electrostatic property we consider in this study is the first electric moment of the cation-molecule system as a whole[54] which, slightly abusing the nomenclature, will be referred to as total dipole moment (even if this term is only unambiguously defined for a neutral system). To keep the study of different methods (and ion-molecule systems) within a manageable limit, we will restrict to cases where all polarizable species (ion and molecule) are modeled with the same method. Indeed one could treat each polarizable site with different methods[55] but it is to be expected that, given the essentially similar nature of the various methods available, such approach would not change the essence of our conclusions. Therefore, in this study we compare the accuracy of PD and SH methods, applying them to the whole ion-molecule system. We present the results obtained for a set of mono- and bivalent cations: Li^+, Na^+, Mg^{2+}, and Ca^{2+}. A basic characteristic is that both ionic polarizability and radius increase in the group, and decrease as the ionic charge increases[56–58] (see Table III).

The work of Alfredsson *et al.*[27] for a water dimer is illustrative of the novel features that the study of ions brings in. As the water dimer separation is varied the PDM faithfully represents the total dipole moment of the system at all physically reasonable distances.[27] In Refs. 47 and 53, though, it was shown that if a water molecule is displaced in the vicinity of a point charge, the PDM (and other schemes as well) is not able to reproduce the nonlinear increase in dipolar moment obtained in *ab initio* calculations at intermediate and contact separations. While this effect is modest for univalent ions, it becomes more important as the ion charge/molecular polarizability increases. In Refs. 47 and 53 it was

TABLE II. CCl_4 parameters for the methods studied.

Point dipoles			Shell model	
	Ref. 68	PD-CCl_4		SH-CCl_4
d_{CCl} (Å)	1.766	1.766	d_{CCl} (Å)	1.766
α_C (Å^3)	0.878	−1.000	k_C (kJ mol^{-1} Å^2)	0
α_{Cl} (Å^3)	1.910	2.880	k_{Cl} (kJ mol^{-1} Å^2)	13 206.0
$\bar{\alpha}$ (Å^3)	10.52	10.52	$q_{DCl}(e)$	5

TABLE III. Electrostatic properties of point charges and cations. Calculated polarizabilities taken from Refs. 56–58.

	Polarizability (Å^3)	Charge (e)
(+)	0.0	1.0
Li^+	0.028 75	1.0
Na^+	0.148 33	1.0
(++)	0.0	2.0
Mg^{2+}	0.0784	2.0
Ca^{2+}	0.522	2.0

emphasized that, for real ions, these conclusions could only be expected to hold for distances for which the point-charge approximation embedded in a rigid sphere is a reasonable model for the ion. This criterion was quantified as the distance at which the potential energies (computed *ab initio*) for the real ion/molecule and point-charge/molecule start to diverge. The study of cations reported here aims to explore this region, so that two new effects will emerge. First, ion polarizability will contribute to the total dipole moment, although given the characteristic low polarizability of cations this effect cannot be expected to alter the conclusions obtained for point charges. Electronic overlap at separations close to contact, though, will represent a substantial change below the limiting distance referred above and its study constitutes the first main theme of the present work. While in the case of the water dimer[27] no particular feature is found within the range where electronic overlap effects could manifest themselves, this is not the case for cations. A strong damping of the induced dipole moment is found in *ab initio* calculations that the molecular polarization methods are not able to cure without modification, which forces the inclusion of damping schemes: while the neglect of polarization results in underestimations of the dipole moment by roughly a factor of 2, the neglect of damping at short separations results in an overestimation of roughly 30% as well. A detailed discussion of the Thole electric-field damping, its relation with polarization methods, and its fine tuning for different ion-molecule dimers will thus constitute the second main theme of this paper. Basically it will be shown that, when used together with the polarization method of choice, it is possible to satisfactorily reproduce the total dipole moment of the complex for all distances and, simultaneously, for different molecular orientations.

The outline of this article is as follows: in Sec. II we discuss the computational details and the methods used; results and conclusion are given, respectively, in Secs. III and IV, while an Appendix summarizes the Thole method for a set of different "flavors."

II. COMPUTATIONAL DETAILS

Different configurations were considered for the ion-molecule system (see Fig. 1). For each arrangement the distance was varied in an interval of ~5 Å. The closest distance for each configuration was chosen where the potential energy was ≈25 kJ mol^{-1} (≈$10k_BT$ at standard temperature) above the potential-energy minimum. In the case of real ions, it is important to note that the closest approach estimated for the dimer at thermal conditions might be larger than that found in the liquid phase to some extent. In the case of Li^+ the minimum distance reached in *ab initio* molecular-dynamics simulations of the liquid is 1.7 Å,[59] while with the criterium used here we consider distances down to 1.6 Å, which are probably inaccessible in a condensed phase. This fact should be kept in mind in order to properly assess the significance of the results at very short distances.

Regarding the definition for the total dipole moment of the ion-molecule dimer, and given that for charged systems the dipole moment depends on the origin of coordinates,[54] the position of the ion has been taken as the origin of the reference system. In this way, in the limit of zero polarizability for the ion the total dipole moment of the system will be that of the molecule (water or carbon tetrachloride).

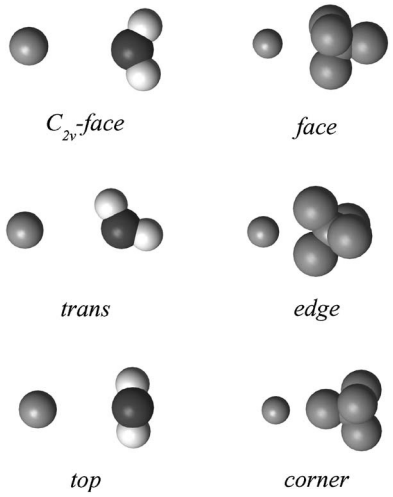

FIG. 1. Configurations studied for the ion-water (left column) and ion-CCl_4 (right column) systems.

A. *Ab initio* calculations

All quantum chemical calculations where performed with the commercial package GAUSSIAN 03. The B3LYP density functional[60] was used with the aug-cc-pvtz basis set.[61,62] For Mg^{2+} and Ca^{2+} we used a modified cc-pVDZ basis set, from which $3s,2p$, and outer shells for Mg^{2+} and $4s,3p$, and outer shells for Ca^{2+} were removed to avoid the charge transfer that otherwise occurs in vacuum at intermediate distances when the M^{2+}–X state becomes less stable than the M^+–X^+ state. Counterpoise calculations with the same density functional and basis sets were done for all the systems to compute the ion-molecule potential energy. The density functional used was chosen because it is known to perform well, with estimated errors of 2% or less for the computed dipole moments and polarizabilities.[63] As a hybrid functional it averages between the underestimation of the polarizability typical of Hartree-Fock calculations and the opposite behavior of pure density functionals. This was also checked by comparing selected calculations with results from Sadlej's basis sets[64,65] and the PBE1PBE functional.[66] The model chemistries used in our calculations are demonstrated to be accurate also in the evaluation of other quantitites of interest.[67]

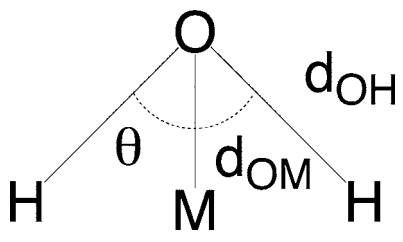

FIG. 2. Geometrical parameters for the water molecule. Site M is represented out of scale for the sake of clarity in the drawing.

B. Polarization methods

A detailed description of polarization methods was given in Ref. 47. Here we just outline the main features of the two methods used in this work. In the point-dipoles method, a polarizability α is associated to one or more sites.[68] The total electric field acting on each site is produced by the external partial charges ($\mathbf{E}^o$) and by both the intramolecular and external induced dipole moments,

$$\mathbf{E}_i = \mathbf{E}_i^o + \sum_{j \neq i} T_{ij} \cdot \mathbf{p}_i, \tag{1}$$

where T_{ij} denotes the dipole field tensor, which for a point dipole located at the origin can be written

$$T = 3\frac{\mathbf{rr}}{r^5} - \frac{I}{r^3}. \tag{2}$$

The induced point dipole on site i is obtained from the total field according to

$$\boldsymbol{\mu}_i = \alpha_i \mathbf{E}_i, \tag{3}$$

and can be computed iteratively until a given threshold of convergence for the induced dipole is reached (we refer to Ref. 5 for issues concerning the efficiency of the different methods for liquid state simulations).

The shell model (also known as Drude oscillator or charge on spring model, see Ref. 5 for suggested nomenclature) is based on a similar approach. Again, a polarizability is assigned to one or more sites. These sites are composed of two charges: one is fixed while the other (q_D) is free to move, linked to the first one via a spring. The sum of both charges is equal to the charge of the atomic site. The spring constant is related to the charge on the moving shell and to the polarizability of the site,

$$k_D = q_D^2/\alpha. \tag{4}$$

An advantage of this method is that it is easy to implement in typical molecular-dynamics codes, while an important drawback is that it increases the number of interaction sites and therefore the number of relative distances to be computed.

In Ref. 47 we reparametrized standard models for both methods; the values of site polarizabilities were fitted in order to reproduce (i) the polarizability tensor of the molecules and (ii) the distance dependence of the total dipole moment in the presence of a point charge.

C. Damping functions

As it will be shown in this paper, a basic finding is that the methods explored in Refs. 47 and 53 are unable to reproduce the substantial decrease of the total dipole moment at distances close to contact which is obtained in *ab initio* calculations. A way to deal with this limitation is the inclusion of electrostatic damping, which can be achieved through a reparametrization of the Thole method.[69] In this seminal work it was recognized that in the interacting point-dipoles model[68] there is a too sharp variation of molecular polarizability with interatomic distances. This is usually illustrated with the diatomic molecule (AB) case, for which the parallel and normal components of its polarizability are proportional to $1/(1-\alpha_A\alpha_B/r^6)$. For $r=(\alpha_A\alpha_B)^{1/6}$ the molecular polarizability diverges and therefore it will be unphysically high in its neighborhood as well. Thole proposed to address this problem using charge distributions instead of point charges, which result in a damping (see below) of the electric field created by point charges and/or point dipoles. The extent of this damping was fitted so that the experimental polarizabilities of a given set of molecules were reproduced satisfactorily. While the mathematical framework will be adopted with few changes, an important difference will be that the method will be implemented recoursing to *ab initio* calculations. The rationale is that given that the method will be applied to *intermolecular* interactions, it is not to be expected that the same parameters found for intramolecular interactions will be optimal in this context, although in some cases it has been transferred without modification to liquid phase simulations due to its ability to eliminate polarization divergences. Here the method will be parametrized so that the *ab initio* dipole moment of the dimer is reproduced all along the ion-molecule distance (with particular emphasis at contact separations) *and* for several orientations of the molecule. This stringent condition is meant to provide some confidence in that the resulting models are physically sound for their use in liquid phase simulations.

A mathematical derivation of the Thole method,[69] that impinges on the pair additive nature of this approach and on the fact that it is not logically connected with polarization, is given in the Appendix. Here we just give the fundamental formulas required for its implementation. Basically, Eqs. (1)–(3) retain their validity with the only change being that both the electric field created by a fixed charge and/or that created by a point dipole (depending on the molecular model) are/is damped by functions $f_1(r)$ and $f_2(r)$,

$$\mathbf{E}^o = f_1(r) q \frac{\mathbf{r}}{r^3}, \tag{5}$$

$$T = f_2(r) 3\frac{\mathbf{rr}}{r^5} - f_1(r)\frac{I}{r^3}. \tag{6}$$

In the limit of *point* charges and/or *point* dipoles we have $f_1(r)=f_2(r)=1$, and the usual expressions are recovered. If on the contrary they are thought to be spatially extended, the form of the damping depends on the charge distribution assumed. Thole concluded that a linear decrease of charge density (up to a cutoff a) was rather ideal for the purpose it had been designed for (fitting of the molecular polarizability). In this approximation we have for the damping functions (see Appendix)

$$f_1(r) = 4\left(\frac{r}{a}\right)^3 - 3\left(\frac{r}{a}\right)^4, \tag{7}$$

$$f_2(r) = \left(\frac{r}{a}\right)^4, \tag{8}$$

up to the cutoff a (for $r>a$ we simply use the pointlike expressions for the fields). As noticed by Bernardo *et al.*,[20] the somewhat pathological behavior at $r=a$ might be problematic in molecular-dynamics simulations. Although *ad hoc*

corrections are possible,[20] they complicate the resulting expressions and therefore, other distributions might be more convenient. The most popular alternative seems to be an exponential distribution[28,36,69] (see Appendix), for which the correction factors are

$$f_1(r) = 1 - e^{-(r/a)^3}, \tag{9}$$

$$f_2(r) = 1 - \left[1 + \left(\frac{r}{a}\right)^3\right] e^{-(r/a)^3}. \tag{10}$$

Finally, while the latter two distribution functions have already been used in the literature, we have also explored the capabilities of using a Gaussian distribution function for each charge (see Appendix), given the good performance that such distributions have shown in electronic structure theory. In this approximation the interaction energy has a simple form (as compared for instance with that of an exponential distribution) at the cost of somewhat more complicated correction factors,

$$f_1(r) = \mathrm{erf}\left(\frac{r}{a}\right) - \frac{2}{\sqrt{\pi}}\left(\frac{r}{a}\right) e^{-(r/a)^2}, \tag{11}$$

$$f_2(r) = \mathrm{erf}\left(\frac{r}{a}\right) - \frac{2}{\sqrt{\pi}}\left(\frac{r}{a}\right) e^{-(r/a)^2}\left[1 + \frac{2}{3}\left(\frac{r}{a}\right)\right]. \tag{12}$$

In any of the above possibilites a plays the role of the characteristic distance of maximum approach. This is particularly clear in the example of two charges "dressed" with Gaussian distributions (described in the Appendix), where it is shown that a is roughly equal to the sum of the widths of both Gaussians [see Eq. (A2)]. Obviously the precise value will depend on the functional form chosen, but will be rather similar in all cases (as will be shown in the paper) and close to the sum of atomic radius as one would expect. It should be noted that in the present approach no use of the scaling concept introduced by Thole is made. The original approach would assume the following relation:

$$a = w(\alpha_1 \alpha_2)^{1/6}, \tag{13}$$

where α_i denotes the polarizatility of each member of the pair and w was assumed to be a universal adimensional scaling parameter, independent of the pair. While such scaling did work in order to fit the molecular polarizability of a set of molecules, it does not seem possible to extend its validity to the intermolecular interactions studied here. Neither the original value of w, nor any optimization, are able to cope with the stringent requirements described above (reproducing the *ab initio* induced dipole moment for all distances and molecular orientations). In addition, such assumption [Eq. (13)] is to some extent a source of confusion as it may lead to the idea that the method is dependent on atomic polarizabilities, while indeed (as shown in the Appendix) the relevant physical parameter is the atomic radius. It is the generally monotonic dependence of polarizability on the atomic radius which makes these two rather different concepts approximately interchangeable for numerical purposes.

Regarding the flexibility of the method, the above possibilities illustrate the potentially unending variety of functional forms from where to choose from. In addition, the a parameter, as just discussed, can be made dependent on each different pair. In this connection, while the formulas given assume the same value of a for the charge and for the dipole, this is not a necessary condition.[28] If a site contains both a charge and a dipole (a typical scenario for many molecular models), its interaction with an external charge and/or dipole can be characterized by different values of a for the charge-charge interaction, dipole-charge interaction, etc. Despite this potential, in the present case of ion-molecule interaction (which is probably one of the most demanding, particularly for doubly charged ions) it has not been necessary to recourse to such possibility, and the value of a for a given pair of sites is in all cases taken to be unique, i.e., independent of the interaction class. Finally, in the cases that have been studied, a is very close to the simple sum of atomic radius, therefore easing considerably the task of developing parameter sets for different pairs.

We close this section emphasizing that this electric-field damping scheme is totally independent of the polarization method used. If, for instance, this approach is used in combination with a point-charge model of polarization (shell method or fluctuating charges) only Eq. (5) is required. If, on the other hand, the molecular model uses point charges and point dipoles (such as in the point-dipole method) one should use both Eqs. (5) and (6).

III. RESULTS

A. Dimer potential energy

For each configuration considered (see Fig. 1) the potential energy has been computed as a function of the ion-molecule distance. In Fig. 3 we show the results for the C_{2v} *face* configuration of the ion-water system and those of the *edge* configuration for the ion-CCl_4 system; similar profiles are found for the other configurations of both systems (not shown). As can be expected, with decreasing ionic radius, the equilibrium distance gets smaller and the well depth increases. This happens both for mono- and divalent cations. The well depth for divalent ions is at least twice that of monovalent ones (in the case of, the highly polarizable, CCl_4 the ratio is of roughly a factor of 4 for ions of similar ionic radius, e.g., Na^+ and Ca^{2+}). The comparison with the point charge is also given. At large distances the potential-energy curves are identical, while at intermediate distances the curves diverge from each other. In principle the breakdown of the point-charge approximation should take place at distances directly related to the ion dimension. This simple rule is indeed valid for cations of the same group, but does not apply between different rows of the periodic table. One would expect that, since the ionic radius of second group cations is smaller or comparable to that of the first group, the point-charge approximation would hold for smaller distances. Contrary to this notion, we notice that it holds down to shorter distances for monovalent than for divalent ions [compare panels (a) and (c) respectively with (b) and (d) of Fig. 3]. This effect can be rationalized in terms of the higher attraction exerted by the double charge on the molecular electronic cloud (as reported in Ref. 47 the dipole moment

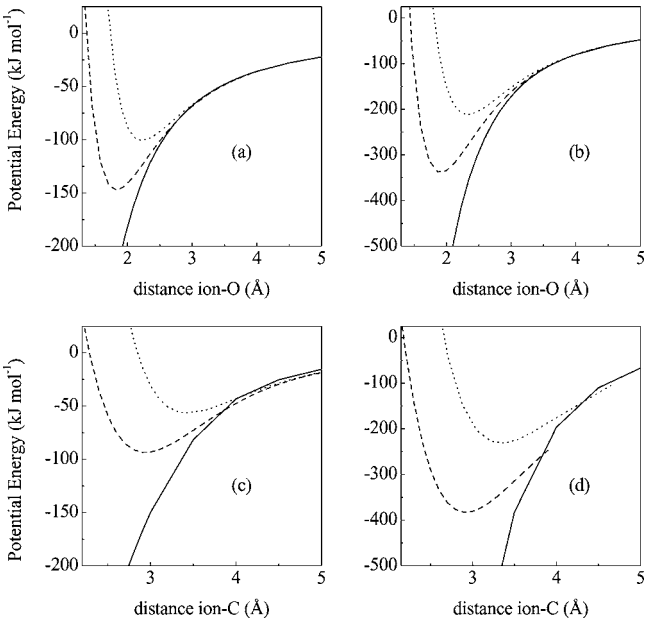

FIG. 3. Potential energy for the C_{2v} face configuration of (a) monovalent and (b) divalent ion-water systems, and for the edge configuration of (c) monovalent and (d) divalent ion-CCl_4 systems. The solid line is used in all panels for point charges. Panels (a) and (c): Li^+ (dashed line) and Na^+ (dotted line). Panels (b) and (d): Mg^{2+} (dashed line) and Ca^{2+} (dotted line). The values for the contact distance of each ion and configuration are reported in Tables IV and V.

induced from a double charge is more than double of the one induced by a single charge). As a consequence the molecular electronic cloud is more shifted towards the cation and interacts with the ion outer shell more strongly than for the monovalued ion (for a given ion-molecule distance).

Finally, the distance where the repulsive energy is above the potential-energy minimum more than 25 kJ mol^{-1} is considered as the lower limit for our calculations. Shorter distances will rarely be found in liquid state simulation. In Tables IV and V we report, respectively, the minimum distances obtained and the well depths for all configurations of each system.

B. Induced dipole moments

The total *ab initio* dipole moments for the ion-molecule complex are depicted in Figs. 4 and 5. The results for a point charge are almost identical to those of "real" cations down to rather small distances: ≈2.5 Å for water, and down to

TABLE IV. Minimum distances considered for each system and configuration [units in angstroms (Å)].

	H_2O			CCl_4		
	Face	*trans*	Top	Face	Edge	Corner
(+)	1.6	1.6	1.6	2.1	2.5	3.7
Li^+	1.6	1.6	1.6	2.1	2.5	3.7
Na^+	1.9	1.95	2.05	2.5	3.0	4.1
(++)	1.7	1.75	1.85	2.2	2.6	3.8
Mg^{2+}	1.7	1.75	1.85	2.2	2.6	3.8
Ca^{2+}	2.1	2.1	2.2	2.5	3.0	4.0

TABLE V. Potential-energy minimum for each system and configuration (units in kJ mol^{-1}).

	H_2O			CCl_4		
	Face	*trans*	Top	Face	Edge	Corner
Li^+	−147.61	−84.91	−87.86	−85.34	−93.48	−34.26
Na^+	−100.71	−54.26	−53.08	−55.78	−56.46	−18.29
Mg^{2+}	−337.75	−218.80	−226.11	−386.45	−382.79	−248.91
Ca^{2+}	−211.05	−126.36	−115.93	−238.96	−230.98	−144.70

≈3.5 Å in the case of CCl_4 [for CCl_4 close to a divalent ion, Fig. 5(b), this distance is increased to ≈4.5 Å]. However, a dramatic difference exists at shorter distances: the dipole moment for a point charge keeps increasing with decreasing distance while for the ions this increase is considerably slowed down and, eventually, a turnover is reached, beyond which the dipole moment decreases with decreasing distance (notice that the results are only displayed up to maximum approach distance as defined above with an energetic criterium, which results for instance in that in some cases the turnover is not reached and only the slowdown of the dipole increase is observed). It is to be noted that the distances at which such effects occur correspond to those typical of molecules within the first solvation shell of the ion in the liquid state,[70] and therefore it does not seem advisable to neglect them.

It is important to understand the physical origin of the total dipole damping. To illustrate the discussion we take for

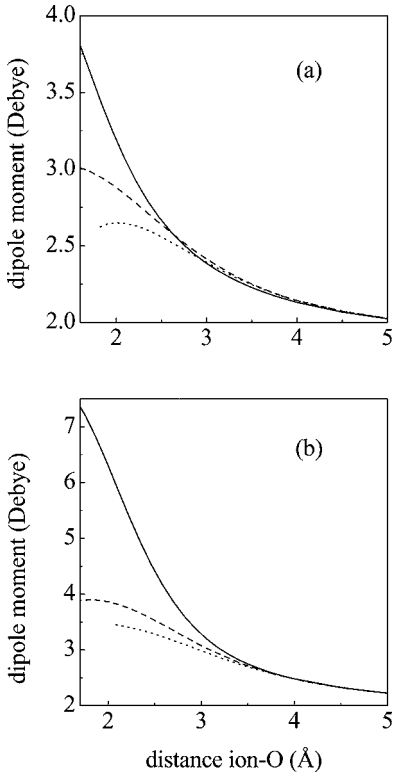

FIG. 4. *ab initio* electric moment for the trans configuration of cation-water dimer. Results for (a) monovalent point charge (solid line), Li^+ (dashed line) and Na^+ (dotted line), and (b) divalent point charge (solid line), Mg^{2+} (dashed line) and Ca^{2+} (dotted line).

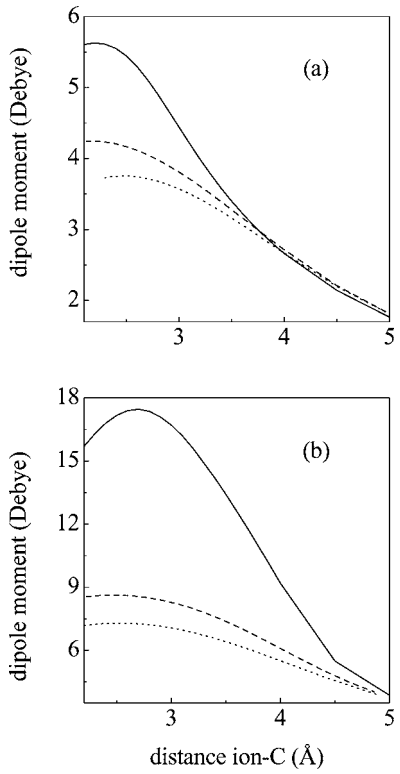

FIG. 5. *ab initio* electric moment for the face configuration of cation-CCl_4 dimer. Results for (a) monovalent point charge (solid line), Li^+ (dashed line) and Na^+ (dotted line), and (b) divalent point charge (solid line), Mg^{2+} (dashed line) Ca^{2+} (dotted line).

instance the C_{2v} face configuration of water (first configuration in Fig. 1). As the molecule approaches the ion, the total dipole is expected to grow mostly due to molecular polarization, with a small contribution from the cation polarization. Given that the molecular dipole is oriented to the right (which we will consider the positive direction), the induced dipole on the ion will also be directed to the right (or, in terms of the shell model, the auxiliary negative charge harmonically bonded to the positive ion site will be shifted to the left). Both effects (increase of the ionic and molecular dipoles with decreasing distance) can be mimicked by any polarization method (except of course the moderate nonlinear increase discussed in Refs. 47 and 53), and therefore should not be a cause of concern to phenomenological molecular polarization methods.

If the ion-molecule distance is reduced to contact, though, a different mechanism sets in as evident from the *ab initio* calculations: repulsion between the electronic clouds of the ion and the molecule, which can be understood as a "mechanical" polarization.[5,71] For the cation this effect is translated in an additional push to the left of its electronic cloud, i.e., this effect will add to that of the purely electrostatic polarization. In short, the ionic contribution will tend to further increase (nonlinearly) the total dipole moment of the complex. However, given its low polarizability, this effect will not be relevant and is superseded by an electronic shift within the molecule. Indeed, a similar reasoning applied to the molecule leads to the conclusion that its electronic cloud will be shifted to the right and therefore will tend to *reduce* the molecular dipole. Given the much higher molecular polarizability, this will be the dominant effect (a similar conclusion is reached if one considers an inverted orientation for the molecule). To summarize, molecular polarization at contact distances results from two opposite effects: a dipole increase due to the presence of the positive ion's charge (which can in principle be represented by any of the methods discussed for electric polarization), and a dipole decrease due to the mechanical shift of electronic clouds. Unfortunately, the latter effect clearly dominates, as can be seen from the *ab initio* results, and is not contained in any of the polarization methods, which will require *ad hoc* modifications at short distances. It is important to note that the two opposing mechanisms can be linked to two different physical aspects: the dipole increase basically depends on electric polarizability while the dipole decrease due to electronic overlap depends on geometrical parameters (ionic and molecular radii).

In connection with the last point, an additional aspect is to be noted: the damping of the dipole moment increases with increasing ionic radius, as the curves get lower along the series (Li^+ and Na^+ or Mg^{2+} and Ca^{2+}). This behavior is common to the most probable configurations of both H_2O and CCl_4 (Figs. 4 and 5), and is a corollary of the previous discussion: for a fixed ion-molecule distance the molecular electronic cloud will have a higher overlap with ions of larger radius. This will result in a stronger shift of this cloud and, therefore, in a smaller molecular dipole. This secondary effect has important consequences for the construction of damping methods. It is possible to imagine a convenient damping model (in terms of ease of simulation) which includes a damping of the electric field felt by the molecule if this field is larger than some threshold, irrespective of the origin of this electric field. In this way it is in principle possible to mimick the dipole decrease with increasing electric field (i.e., proximity to the ion). Unfortunately, the dependence on the ion just discussed makes such a simple approach only approximate at best: we find for instance that while the positive charge on Li^+ and Na^+ create the same field on the molecule, the polarization induced at contact differs substantially. In consequence a damping of the field of this sort might work for one ion but would not do for other ions. The damping method should thus take into account geometric aspects. In its simpler form it should depend on the ion and molecule radii, and this is where the Thole method comes in, as it is based on the inclusion of mutual size effects on the computation of the electric field at short separations.

C. Performance of undamped methods

Before exploring the utility of this damping method, we analyze the shortcomings of the uncorrected polarization methods in the light of the two mechanisms just discussed. Only the results for a single configuration and for the molecular polarization models that performed better for the point-charge model of the ion will be shown (the behavior is highly similar for other configurations and models). The unability of the unmodified point dipole and shell methods to reproduce the dipole moment at small distances is manifest in Fig. 6 for water and in Fig. 7 for carbon tetrachloride. The

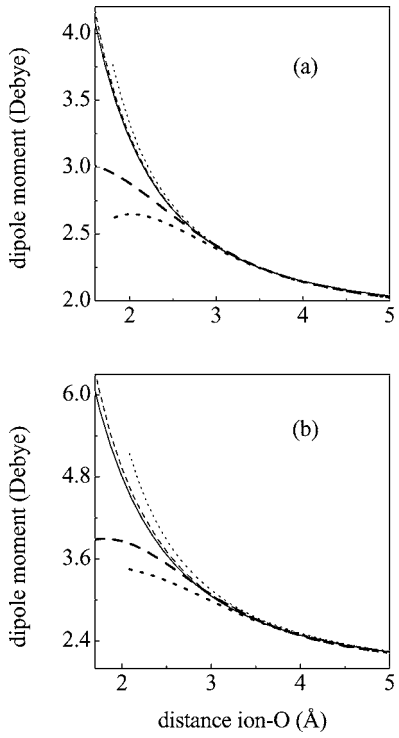

FIG. 6. Electric moment for the *trans* configuration of the cation-water dimer. Thick lines are for *ab initio* calculations and thin lines are for PD2-H_2O curves. Results for (a) monovalent point charge (solid line), Li^+ (dashed line) and Na^+ (dotted line), and (b) divalent point charge (solid line), Mg^{2+} (dashed line) and Ca^{2+} (dotted line).

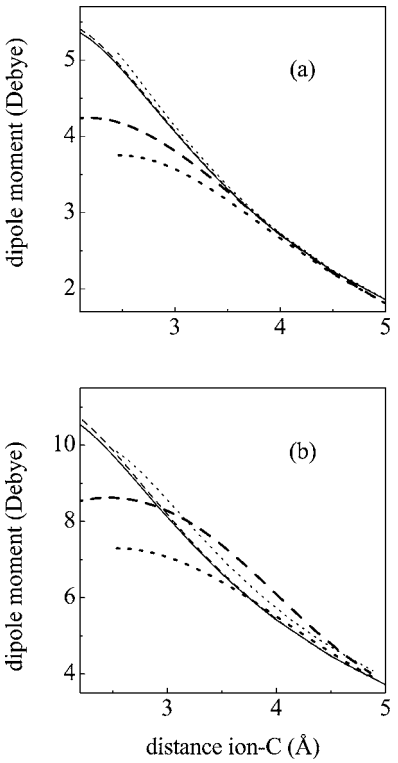

FIG. 7. Electric moment for the face configuration of the cation-CCl_4 dimer. Thick lines are for *ab initio* calculations and thin lines are for PD-CCl_4 curves. Results for (a) monovalent point charge (solid line), Li^+ (dashed line) and Na^+ (dotted line), and (b) divalent point charge (solid line), Mg^{2+} (dashed line) and Ca^{2+} (dotted line).

fundamental problem is that the total dipole of the complex is predicted to grow monotonically as the distance is reduced, in contrast with the already discussed damped increase (followed by a turnover) of the *ab initio* results.

The case of water close to a monovalent ion [Fig. 6(a)] can serve to illustrate the main features. First, it is evident that the differences at contact separations are quantitatively important even for this case of low ionic charge/low molecular polarizability: for Li^+ there is a 40% difference between the dipole moment predicted by the polarizable model and the *ab initio* result. Second, the effect of ion polarizability is minor: the curves for Li^+ and Na^+ are rather close to each other and to the curve that corresponds to a point charge. This feature illustrates the feeble effect of the dipole moment induced on the ion as compared with the molecular induced dipole. In connection with the two mechanisms described in Sec. III B, we see how the curves are slightly steeper as the ion's polarizability increases, i.e., the predicted polarization is slightly higher for the case of Na^+ than for Li^+ due to the higher ionic polarizability of the former, which illustrates that the polarization methods only take into account this sort of ion-dependent polarization. As was described in Sec. III B, there is no electronic overlap effect included, while it is precisely this finite-size effect which results in the *ab initio* results showing exactly the opposite trend, i.e., the induced dipole is smaller for the Na^+ case than for Li^+. The same basic trends are found for all cases studied (see Figs. 6 and 7). One can notice for instance that for divalent ions close to water [Fig. 6(b)] the differences are qualitatively very similar, although quantitatively larger. For carbon tetrachloride the scenario is rather similar to that of water as well [Figs. 7(a) and 7(b)]. Again, the *ab initio* results show the opposite trend of classical methods: the dipole moment of the system lowers as the ion polarizability increases.

D. Polarization plus Thole damping

Section III C makes evident the need for a damping scheme. This can be achieved to a great extent by using the Thole method described in Sec. II C and the Appendix. As shown there, this method can be implemented in different flavors, which depend on the chosen joint charge distribution: linear [LIN, Eqs. (7) and (8)], exponential [EXP, Eqs. (9) and (10)], or Gaussian [GAUSS, Eqs. (11) and (12)]. Any of the three can be used in conjunction with the point dipoles or shell models of polarization. It will be shown that once the parameter on which they depend (a) is optimized for each distinct pair, every possible combination of polarization and damping method performs reasonably well.

Figure 8 illustrates the performance of the different combinations for the Li^+-water dimer, which will be the center of most of the discussion. Panels (a) and (b) correspond to PDM and SH, respectively. The crucial point to observe is that the three damped curves closely follow the *ab initio* results, resulting in a much better performance with respect to the undamped models. While only a subset of the results will be shown, this behavior is also found for the rest of the ions, for the different molecular orientations studied (see Fig. 1), and for the CCl_4 molecule as well. Coming to the finer level of detail, the PDM-LIN and SH-LIN give the best re-

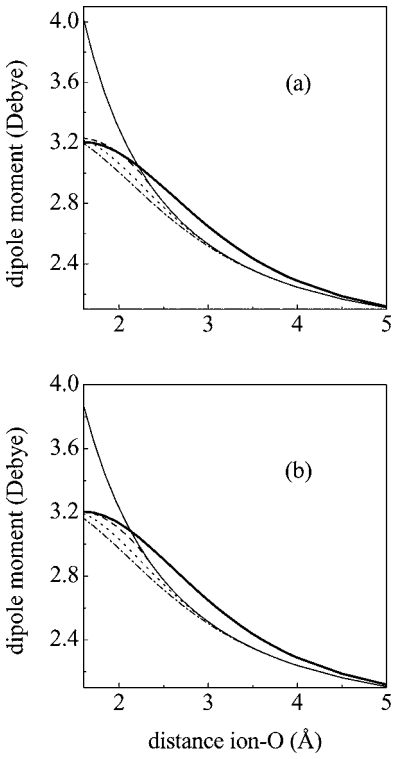

FIG. 8. Comparison among the methods discussed in the text for the C_{2v} face configuration in the Li^+-water dimer. Panel (a): PDM-H_2O (thin solid line), PDM-LIN (dashed line), PDM-EXP (dotted line), and PDM-GAUSS (dash-dot line). Panel (b): SH-H_2O (thin solid line), SH-LIN (dashed line), SH-EXP (dotted line), and SH-GAUSS (dash-dot line). The thick solid line in both panels is used for *ab initio* results.

sults, followed by the EXP distribution, and with GAUSS coming last. Indeed, the LIN distribution was showed to be the best performing scheme for all the ions considered (in the case of water); the results are shown in Fig. 9. We now discuss in more depth some additional aspects of the fits.

First, it can be noticed that for each method (LIN, EXP, and GAUSS) the corresponding curves are almost equal in panels (a) and (b) of Fig. 8, i.e., each charge distribution performs equally well for any of the two polarization methods (point dipoles or shell). The almost imperceptible differences can be ascribed to two factors: (i) the PD method includes a damping of the dipolar interaction while in SH only the charge-charge interaction is damped (indeed the high similarity between the curves illustrates the feeble contribution of the dipole field damping); (ii) since in the SH model, the shell charge is displaced with respect to the zero-field position, the (distance-dependent) damping will be slightly different from the one used for PD (where the charges remain fixed).

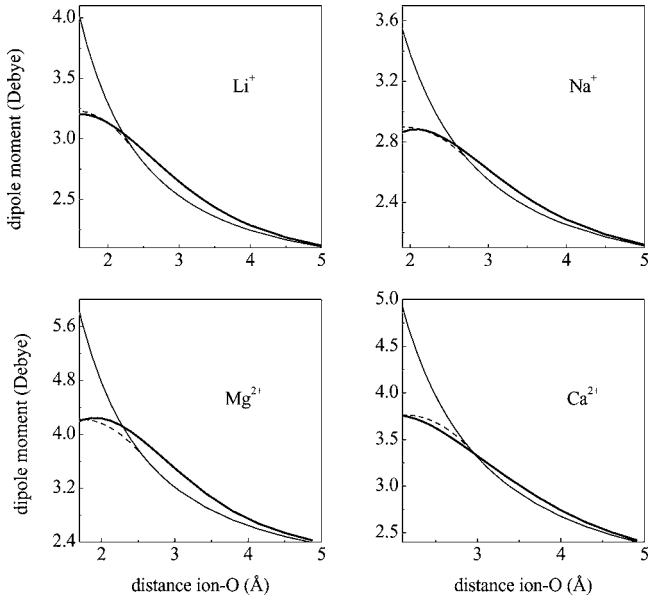

FIG. 9. Total electric moment for the C_{2v} face configuration of the ion-water system; *ab initio* results (thick solid line), PDM-H_2O (thin solid line), and PDM-LIN (dotted line).

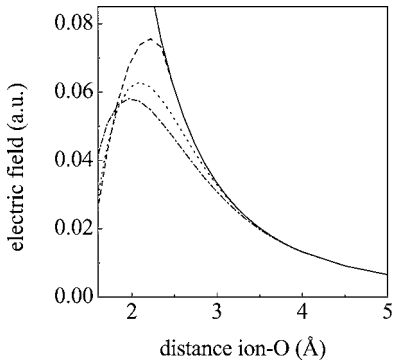

FIG. 10. Distance dependence of the total electric field on the ion; PDM-H_2O (solid line), PDM-LIN (dashed line), PDM-EXP (dotted line), and PDM-GAUSS (dash-dot line).

Second, while the three schemes are able to satisfactorily reproduce the *ab initio* results at short distances, the underestimation found in Refs. 47 and 53 at intermediate distances ($2.2 < r < 4$ Å) is left unchanged. This drawback derives, as discussed in Refs. 47 and 53, from the fact that the polarization methods studied are linear and thus cannot reproduce the system hyperpolarizability obtained with quantum chemical calculations. The present implementation of the Thole damping cannot be a solution for this either, as a larger polarization is required instead of a damping (although it is possible to imagine that this deviation might be tackled with more complex charge distributions). This limitation, though, should not be overemphasized; the worst disagreement for any of the different combination of methods yields a relative error in the range of 5%–6% of the total dipole moment (the largest deviation occurs for the unprobable *top* configuration, see Fig. 1, and does not exceed a 10%), which justifies limiting the present study to the simple charge distributions described. For the linear and exponential cases the deviation takes place close to 3 Å, i.e., in the region where there is still no damping, and can thus be totally ascribed to the lack of hyperpolarizability. For the Gaussian method, the largest deviation ($\approx 6\%$) occurs at ≈ 2.5 Å, and thus also includes a small contribution from an (undesired) nonzero damping in this region.

The latter point highlights how the damping differs somewhat between different charge distributions. It is possible to get some additional insight by considering the total electric field felt by the ion. Figure 10 displays the results for both damped and undamped calculations within the physi-

TABLE VI. Parameter a used for the ion-oxygen interaction (in angstroms) for the linear, exponential, and Gaussian dampings. The radius (a_{IO}^{est}) estimated from the experimental values of the atomic radius is reported in the last column.

	LIN	EXP	GAUSS	a_{IO}^{est}
Li^+	2.59	1.79	1.44	1.63
Na^+	2.98	2.05	1.64	1.79
Mg^{2+}	2.79	1.92	1.57	1.65
Ca^{2+}	3.13	2.14	1.72	1.81

cally meaningful range of distances. The main feature of the LIN scheme (the one that produces better results) is that it stays close to the undamped curve down to a shorter distance than the EXP or GAUSS distributions. The larger steepness of this damping seems thus to be important in order to get a better fit. Nevertheless, since the present results are rather satisfactory, a marginal improvement along these lines has not been pursued.

Regarding the precise values for the a_{ij} parameters (with i denoting an ion and j an atomic site within the molecule), in the case of water *only* the cation-oxygen interaction was damped, while the cation-hydrogen interaction was left unchanged, so that a single parameter is needed for each ion (a_{IO}). The results are summarized in Table VI. As a result of the fitting, a_{IO} has the nice characteristic of being independent of the polarization method used (point dipoles or shell method). The last column contains the estimated value for a_{IO}, calculated as $a_{IO}^{est}=(r_{ion}^2+r_O^2)^{1/2}$ [see Eq. (A2)], where r_{ion} and r_O denote, respectively, the ionic radius[72–75] and the oxygen van der Waals radius.[76] For the GAUSS distribution the fitted values are very close to the estimated ones: as a rule of thumb the fitted ones are ≈10% lower than the estimated ones. This approximate rule also applies for the CCl_4 results (Table VII), and could thus be used as a reasonable estimate if the method should be applied to other atomic sites. For the EXP distribution the fitted values are ≈15% higher than the estimated ones, while for the LIN distribution they are consistently higher by ≈70%.

So far the discussion has been mainly centered on the water molecule; for carbon tetrachloride the results are rather similar although some differing details have to be considered. The a_{ij} parameters were fitted for both the ion-chlorine and ion-carbon interactions (Table VII). Contrary to the case of water, for this system the EXP scheme is not the one that performs better although, as it was clear in the case of Li^+-water, the differences are rather minor. The results for the PD-EXP models are displayed in Fig. 11, showing features similar to those for the water case.

TABLE VII. Parameter a (in angstroms) used for the ion-chlorine (a_{Cl}) and ion-carbon (a_C) interactions; values for the linear, exponential, and Gaussian dampings. The radius (a^{est}) estimated from the experimental values of the atomic radius is reported in the last two columns.

	LIN		EXP		GAUSS		a^{est}	
	a_{ICl}	a_{IC}	a_{ICl}	a_{IC}	a_{ICl}	a_{IC}	a_{ICl}	a_{IC}
Li^+	3.05	2.8	2.0	1.8	1.6	1.5	1.85	1.80
Na^+	3.65	2.9	2.28	1.9	1.84	1.7	1.99	1.95
Mg^{2+}	3.0	2.7	1.9	1.4	1.6	1.5	1.87	1.82
Ca^{2+}	3.46	3.0	2.35	2.0	1.9	1.9	2.01	1.97

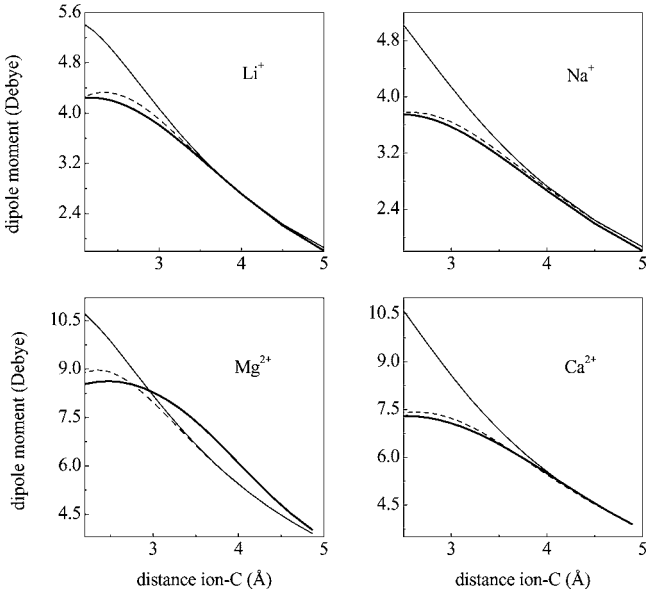

FIG. 11. Total electric moment for the face configuration of the ion-CCl_4 system; *ab initio* results (thick solid line), PD-CCl_4 (thin solid line), and PD-EXP (dashed line).

IV. CONCLUDING REMARKS

The aim of this work has been to explore the possibility of reproducing the mutually induced dipole moment of a molecular complex with simple phenomenological methods that can be easily implemented in molecular dynamics codes. This has been done in a demanding environment such as that corresponding to polarizable molecules in the presence of polarizable cations, using high-level *ab initio* results as a benchmark. It has been shown that a reparametrization of the Thole electric-field damping method, combined with almost any simple polarization method, is able to reproduce rather satisfactorily the induced dipole moment of the cation-molecule dimer. This has been demonstrated for several (mono- and divalent) cations, molecules (water and carbon tetrachloride), and for an extended set of molecular orientations and ion-molecule distances. The largest deviations are due to the nonlinear behavior at intermediate separations, although in no case these reach 10% of the total dipole moment, and therefore it does not seem necessary to resort to more sophisticated charge densities. The study of this approach for anions (with the increased complexity that stems from their higher polarizabiity) and to clusters larger than the dimer will constitute stringent tests of the present approach.

Finally, the present work can be regarded as a preliminary step for a novel strategy in the development of a force field. The usual route has been to include a simple polarization method within a typical nonpolarizable force field, and subsequently fine tune the parameters using for instance *ab initio* results for the energy of clusters and/or thermodynamic properties for condensed phase, etc. A first casualty of such an approach is that there is no guarantee that the resulting

dipole moment (a crucial quantity for the calculation of spectra) is physically meaningful. Moreover, the divergent behavior shown here for simple polarization methods at short distances can be a source of an undesired strain on the whole force field: the important overestimation of the Coulomb interaction forces a consequent damping by other pair additive terms (such as Lennard-Jones parameters), which might not work properly in all environments. In short, it seems more advisable to first construct a polarizable electrostatic model recoursing to *ab initio* calculations and, in a second stage, to include additive terms in order to develop a force field that reproduces the potential-energy landscape.

ACKNOWLEDGMENTS

This work was supported by EC TMR network (HPRN-CT-2000-19), MCYT project (BFM2001-2077), a grant of Regione Autonoma della Sardegna, and an Austria-Spain coordinated action.

APPENDIX

Here we summarize the basic aspects of the Thole method. It should be recognized at the outset that, despite the fact that this theory was developed to improve the point-dipole method of molecular polarizability, it has no direct connection with polarization. Indeed it could be described as a theory to substitute a set of point charges by a corresponding set of rigid charge distributions, neglecting any induced deformation due to mutual interaction (polarization). In fact, related schemes were developed,[77] for example, to replace a point-charge nucleus by a finite-size nucleus in Dirac-Fock calculations.[78–80] The final result is a scheme in which the pair additive nature is maintained and the fields at contact separation between pairs of charges are damped due to their finite extent. It is this damping of the electric field which, when used in conjunction with a polarization method of choice, results in a corresponding damping of the induced dipole.

The method can be motivated by the form of the interaction energy between two Gaussian charge distributions, a well-known case in electronic structure theory. The distributions are taken to have total charges q_1 and q_2, respectively, so that they can be written in terms of normalized (N) Gaussians [$\rho_1(r)=q_1\rho_1^N(r)$ and $\rho_2(r)=q_2\rho_2^N(r)$]. The total interaction energy is[81,82]

$$U = q_1 q_2 \int\int \frac{\rho_1^N(r_1)\rho_1^N(r_2)d\mathbf{r}_1 d\mathbf{r}_2}{r_{12}} = q_1 q_2 \frac{\mathrm{erf}(r_{12}/a)}{r_{12}}, \tag{A1}$$

where erf(r) denotes the error function (the Coulomb interaction is recovered in the long-distance limit as this function tends to 1). The parameter a depends on the width of each of the Gaussians by the simple relation

$$a = \sqrt{a_1^2 + a_2^2}, \tag{A2}$$

with the normalized three-dimensional Gaussian being

$$\rho^N(r) = (\pi a^2)^{-3/2} e^{-(r/a)^2}. \tag{A3}$$

Thole's method is based on the observation that Eq. (A1) can be interpreted as resulting from the interaction of a point charge (q_1) with a distributed charge (q_2), which creates a potential of the form $V(r)=q_2\varphi(r;a)$ [in this case $\varphi(r;a)=\mathrm{erf}(r/a)/r$]. It should be noted that this potential depends on a parameter (a) which contains information on *both* interacting distributions [reflected in relation (A2) for the gaussian case]. This interpretation can be extended to systems of more than a couple of charges as the theory is pair additive (see the dipole case below for an example).

We can immediately derive the electric field generated by such a distribution,

$$\mathbf{E} = -\nabla[q\varphi(r;a)] = -q\dot{\varphi}\frac{\mathbf{r}}{r} = [-r^2\dot{\varphi}]q\frac{\mathbf{r}}{r^3} \equiv f_1(r)q\frac{\mathbf{r}}{r^3}. \tag{A4}$$

Notice that the following correction has been defined:

$$f_1 = -r^2\dot{\varphi}, \tag{A5}$$

which acts on the field that would be created by a point charge, and which depends on the derivative of the electric potential by unit of charge ($\dot{\varphi}$). The latter function can be related with the charge distribution that creates it by applying Gauss' theorem. For a spherically symmetric distribution

$$\mathbf{E} = \frac{\mathbf{r}}{r^3}\int_0^r 4\pi r^2\rho(r)dr, \tag{A6}$$

which together with Eq. (A4) yields

$$\dot{\varphi} = -\frac{1}{r^2}\int_0^r 4\pi r^2\rho^N(r)dr. \tag{A7}$$

In the original Thole approach one would start by assuming a given functional form for $\rho^N(r)$ (related in a nontrivial way with the unknown atomic distributions of each member of the pair). With this normalized charge density one can compute $\dot{\varphi}$ [Eq. (A7)], and finally the damping of the electric field [Eq. (A5)].

In the form just described Thole's approach can be applied to models with only point charges. Originally, though, it was developed for models for which only point dipoles exist. The extension to this case[28] starts from a finite dipole, with charge $-q$ at the origin plus a charge q at a position $\mathbf{l}$. Each of both charges is assumed to consist of a charge distribution of the type just described above. Therefore, thanks to the mentioned pair additive character of this approach, the interaction with an external charge Q is

$$U = Qq\varphi(r) + Q(-q)\varphi(r') = Qq[\varphi(r') - \varphi(r)]. \tag{A8}$$

The position vector of charge Q with respect to q (denoted $\mathbf{r}'$) can be expressed as $\mathbf{r}'=\mathbf{r}-\mathbf{l}$, which together with a Taylor expansion yields

$$U \cong Qq\,\nabla\varphi\cdot(-\mathbf{l}). \tag{A9}$$

With the usual definition for the dipole moment ($\mathbf{p}\equiv q\mathbf{l}$), the above expression becomes exact in the limit $\mathbf{l}\to 0$,

$$U = -Q\nabla\varphi\cdot\mathbf{p}, \tag{A10}$$

so that the potential created by such a dipole can be identified as

$$\psi = -\nabla\varphi\cdot\mathbf{p}. \tag{A11}$$

Like in the case of a charge, it is now straightforward to derive the electric field it creates,

$$\mathbf{E} = \nabla(\nabla\varphi\cdot\mathbf{p}) = \nabla\nabla\varphi\cdot\mathbf{p} \equiv T\cdot\mathbf{p}, \tag{A12}$$

where the dipole field tensor has been defined ($T \equiv \nabla\nabla\varphi$). Its components can be readily computed

$$T_{ij} = \frac{\partial}{\partial r_i}\frac{\partial}{\partial r_j}\varphi = \frac{\partial}{\partial r_j}\left(\frac{\dot{\varphi}}{r}r_i\right) = \frac{r^3}{3}\left[\ddot{\varphi} - \frac{\dot{\varphi}}{r}\right]3\frac{r_i r_j}{r^5} - [-\dot{\varphi}r^2]\frac{\delta_{ij}}{r^3}$$

$$\equiv [f_2]3\frac{r_i r_j}{r^5} - [f_1]\frac{\delta_{ij}}{r^3}, \tag{A13}$$

from which we conclude that the usual expression [Eq. (2)] is corrected by factors $f_1(r;a)$ [see Eq. (A5)] and $f_2(r;a) = (r^3/3)[\ddot{\varphi} - \dot{\varphi}/r]$

With this general framework, it is now possible to deduce the correction factors corresponding to any joint charge distribution $[\rho^N(r)]$ of choice. Thole favored the use of a linear behavior,

$$\rho^N(r) = \begin{cases} (3/\pi a^3)(1 - r/a) & \text{for } r < a \\ 0 & \text{for } r > a, \end{cases} \tag{A14}$$

which results in the corrections displayed in Eqs. (7) and (8). The corresponding interaction potential can be obtained after integration of this distribution [see Eq. (A7)],

$$\varphi(r) = \begin{cases} 1/r & \text{for } r > a \\ (1/a)[2 - 2(r/a)^2 + (r/a)^3] & \text{for } r < a. \end{cases} \tag{A15}$$

The most popular distribution for molecular-dynamics simulation seems to be an exponential one[28,39,69]

$$\rho^N(r) = \frac{3}{4\pi a^3}e^{-(r/a)^3}, \tag{A16}$$

with the corresponding correction factors displayed in Eqs. (9) and (10), while the interaction potential has a somewhat involved form,[28]

$$\varphi(r) = \frac{1}{r} - \frac{e^{-(r/a)^3}}{r} + \frac{1}{a}\Gamma(2/3)Q\left(\frac{2}{3},\left(\frac{r}{a}\right)^3\right), \tag{A17}$$

where $Q(x,y)$ is the incomplete gamma function.[82]

Finally, we have also included the distribution that has been used to motivate the initial part of this Appendix, characterized by a rather simple form of the interaction potential

$$\varphi(r) = \frac{\mathrm{erf}(r/a)}{r}, \tag{A18}$$

and for which the correction factors that result are displayed in Eqs. (11) and (12). The (so far unknown) joint charge distribution corresonding to this case can be obtained by derivation of Eq. (A7). A three-dimensional normalized Gaussian [Eq. (A3)] is obtained, as should be expected from the very well-known properties of Gaussian pairs.

[1] T. Halgren and W. Damm, Curr. Opin. Struct. Biol. **11**, 236 (2001).
[2] A. van der Vaart, B. D. Bursulaya, C. L. Brooks, and K. K. Merz, J. Phys. Chem. B **104**, 9554 (2000).
[3] S. Patel and C. L. Brooks, J. Comput. Chem. **25**, 1 (2004).
[4] P. Cieplak, J. Caldwell, and P. Kollman, J. Comput. Chem. **22**, 1048 (2001).
[5] S. W. Rick and S. J. Stuart, Rev. Comput. Chem. **18**, 89 (2002).
[6] P. Alström, A. Wallqvist, S. Engström, and B. Jönsson, Mol. Phys. **68**, 563 (1989).
[7] A. Wallquist, P. Alström, and G. Karlström, J. Phys. Chem. **94**, 1649 (1990).
[8] U. Niesar, G. Corongiu, E. Clementi, G. R. Kneller, and D. K. Bhattacharya, J. Phys. Chem. **94**, 7949 (1990).
[9] J. Caldwell, L. X. Dang, and P. A. Kollman, J. Am. Chem. Soc. **112**, 9144 (1990).
[10] H. Saint-Martin, C. Medina-Llanos, and I. Ortega-Blake, J. Chem. Phys. **93**, 6448 (1990).
[11] M. Sprik, J. Phys. Chem. **95**, 2283 (1991).
[12] S. B. Zhu, S. Singh, and G. W. Robinson, J. Chem. Phys. **95**, 2791 (1991).
[13] C. Millot and A. J. Stone, Mol. Phys. **77**, 439 (1992).
[14] L. X. Dang, J. Chem. Phys. **97**, 2659 (1992).
[15] R. E. Kozack and P. C. Jordan, J. Chem. Phys. **96**, 3120 (1992).
[16] A. Wallqvist and B. J. Berne, J. Phys. Chem. **97**, 13841 (1993).
[17] J. W. Halley, J. R. Rustad, and A. Rahman, J. Chem. Phys. **98**, 4110 (1993).
[18] L. X. Dang and D. E. Smith, J. Chem. Phys. **99**, 6950 (1993).
[19] M. Wilson and P. A. Madden, J. Phys.: Condens. Matter **5**, 2087 (1993).
[20] D. N. Bernardo, Y. Ding, K. Krogh-Jespersen, and R. M. Levy, J. Phys. Chem. **98**, 4180 (1994).
[21] S. W. Rick, S. J. Stuart, and B. J. Berne, J. Chem. Phys. **101**, 6141 (1994).
[22] B. J. Palmer, Chem. Phys. **184**, 163 (1994).
[23] D. Borgis and A. Staib, Chem. Phys. Lett. **238**, 187 (1995).
[24] J. C. Soetens and C. Millot, Chem. Phys. Lett. **235**, 22 (1995).
[25] A. A. Chialvo and P. T. Cummings, J. Chem. Phys. **105**, 8274 (1996).
[26] L. X. Dang and T. M. Chang, J. Chem. Phys. **106**, 8149 (1997).
[27] M. Alfredsson, J. P. Brodholt, K. Hermansson, and R. Vallauri, Mol. Phys. **94**, 873 (1998).
[28] J. C. Burnham, J. Li, S. S. Xantheas, and M. Leslie, J. Chem. Phys. **110**, 4566 (1999).
[29] B. Chen, J. Xing, and J. I. Siepmann, J. Phys. Chem. B **104**, 2391 (2000).
[30] H. Saint-Martin, J. Hernandez-Cobos, M. I. Bernal-Uruchurtu, I. Ortega-Blake, and H. J. C. Berendsen, J. Chem. Phys. **113**, 10899 (2000).
[31] K. Ando, J. Chem. Phys. **115**, 5228 (2001).
[32] B. Guillot and Y. Guissani, J. Chem. Phys. **114**, 6720 (2001).
[33] G. Ferenczy and C. A. Reynolds, J. Phys. Chem. A **105**, 11470 (2001).
[34] H. A. Stern, F. Rittner, B. J. Berne, and R. A. Friesner, J. Chem. Phys. **115**, 2237 (2001).
[35] K. H. Cho, K. T. No, and H. A. Scheraga, J. Mol. Struct. **641**, 77 (2002).
[36] P. Ren and J. W. Ponder, J. Comput. Chem. **23**, 1497 (2002).
[37] R. Chelli and P. Procacci, J. Chem. Phys. **117**, 9175 (2002).
[38] H. Yu, T. Hansson, and W. F. van Gunsteren, J. Chem. Phys. **118**, 221 (2003).
[39] P. Ren and J. W. Ponder, J. Phys. Chem. B **107**, 5933 (2003).
[40] G. Lamoreoux and B. Roux, J. Chem. Phys. **119**, 3025 (2003).
[41] E. M. Mas, J. Chem. Phys. **118**, 4386 (2003).
[42] G. A. Kaminski, R. A. Friesner, and R. Zhou, J. Comput. Chem. **24**, 267 (2003).
[43] H. Yu and W. F. van Gunsteren, J. Chem. Phys. **121**, 9549 (2004).
[44] Z. Z. Yang, Y. Wu, and D. X. Zhao, J. Chem. Phys. **120**, 2541 (2004).
[45] T. Yan, C. J. Burnham, M. G. Del Popolo, and G. A. Voth, J. Phys. Chem. B **108**, 11877 (2004).
[46] T. J. Giese and D. M. York, J. Chem. Phys. **120**, 9903 (2004).
[47] M. Masia, M. Probst, and R. Rey, J. Chem. Phys. **121**, 7362 (2004).
[48] V. M. Anisimov, G. Lamoureux, I. V. Vorobyov, N. Huang, B. Roux, and A. D. MacKerell, Jr., J. Chem. Theory Comput. **1**, 153 (2005).
[49] E. V. Tsiper, Phys. Rev. Lett. **94**, 013204 (2005).
[50] E. Harder, B. Kim, R. A. Friesner, and B. J. Berne, J. Chem. Theory Comput. **1**, 169 (2005).
[51] R. Chelli, M. Pagliai, P. Procacci, G. Cardini, and V. Schettino, J. Chem. Phys. **122**, 074504 (2005).
[52] S. Yu. Noskov, G. Lamoureux, and B. Roux, J. Phys. Chem. B (to be published).

[53] M. Masia, M. Probst, and R. Rey, Comput. Phys. Commun. **169**, 331 (2005).
[54] C. J. F. Böttcher, *Theory of Electric Polarization* (Elsevier, Amsterdam, 1973).
[55] S. J. Stuart and B. J. Berne, J. Phys. Chem. **100**, 11934 (1996).
[56] H. Coker, J. Phys. Chem. **80**, 2078 (1976).
[57] W. R. Johnson and K. T. Cheng, Phys. Rev. A **53**, 1375 (1996).
[58] I. S. Lim, J. K. Laerdahl, and P. Schwerdtfeger, J. Chem. Phys. **116**, 172 (2002).
[59] A. P. Lyubartsev, K. Laasonen, and A. Laaksonen, J. Chem. Phys. **114**, 3120 (2001).
[60] A. D. Becke, J. Chem. Phys. **98**, 5648 (1993).
[61] D. E. Woon and T. H. Dunning, Jr., J. Chem. Phys. **98**, 1358 (1993).
[62] K. A. Peterson, D. E. Woon, and T. H. Dunning, Jr., J. Chem. Phys. **100**, 7410 (1994).
[63] D. J. Tozer and N. C. Handy, J. Chem. Phys. **109**, 10180 (1998).
[64] A. J. Sadlej, Collect. Czech. Chem. Commun. **53**, 1995 (1988).
[65] A. J. Sadlej, Theor. Chim. Acta **79**, 123 (1991).
[66] J. P. Perdew, K. Burke, and M. Ernzerhof, Phys. Rev. Lett. **77**, 3865 (1996).
[67] W. Koch and M. C. Holthausen, *A Chemist's Guide to DFT* (Wiley-VCH, Weinheim, 2001), p. 178.
[68] J. Applequist, J. R. Carl, and K. K. Fung, J. Am. Chem. Soc. **94**, 2952 (1972).
[69] B. T. Thole, Chem. Phys. **59**, 341 (1981).
[70] M. Masia and R. Rey, J. Phys. Chem. B **107**, 2651 (2003).
[71] J. E. Hanlon and A. W. Lawson, Phys. Rev. **113**, 472 (1959).
[72] R. D. Shannon, Acta Crystallogr., Sect. A: Cryst. Phys., Diffr., Theor. Gen. Crystallogr. **A32**, 751 (1976).
[73] R. D. Shannon and C. T. Prewitt, Acta Crystallogr., Sect. B: Struct. Crystallogr. Cryst. Chem. **B25**, 925 (1969).
[74] R. D. Shannon and C. T. Prewitt, Acta Crystallogr., Sect. B: Struct. Crystallogr. Cryst. Chem. **B26**, 1046 (1970).
[75] J. E. Huheey, E. A. Keiter, and R. L. Keiter, *Inorganic Chemistry: Principles of Structure and Reactivity*, 4th ed. (Harper Collins, New York, 1993).
[76] A. Bondi, J. Phys. Chem. **68**, 441 (1964).
[77] W. H. Press, S. A. Teukolsky, W. T. Vetterling, and B. P. Flannery, *Numerical Recipes in Fortran 77*, 2nd ed. (Cambridge University Press, Cambridge, England, 1992).
[78] A. K. Mohanty and E. Clementi, Int. J. Quantum Chem. **39**, 487 (1991).
[79] A. K. Mohanty and E. Clementi, Int. J. Quantum Chem. **40**, 429 (1991).
[80] Y. Ishikawa, R. Baretty, and R. C. Binning, Jr., Chem. Phys. Lett. **121**, 130 (1985).
[81] L. Jensen, P.-O. Åstrand, A. Osted, J. Kongsted, and K. V. Mikkelsen, J. Chem. Phys. **116**, 4001 (2002).
[82] T. Helgaker, P. Jørgensen, and J. Olsen, *Molecular Electronic-Structure Theory* (Wiley, Chichester, 2000).